The Iranian Journal of Mechanical Engineering Transactions of ISME
Journal homepage: https://jmee.isme.ir/
Vol. 26, No. 2, 2025, pp. 135-148

Research Paper

DOI: https://doi.org/10.30506/jmee.2025.2051009.1366

Numerical Analysis of Composite Beams with Piezoelectric Actuators

Ramezanali Mahdavinejad[*]
Professor

Taraneh Sheydayi[†]
B.Sc. Student

Arian Ariakia[‡]
B.Sc. Student

This study presents a detailed numerical analysis of composite beams enhanced with piezoelectric actuators, focusing on their mechanical performance under varying design parameters. Finite Element Analysis (FEA) using Abaqus software was employed to investigate the influence of fiber orientation angles (0° to 90°) and the number of layers (2 to 6) on the stress-strain behavior and bending resistance of the beams. The results demonstrate that optimal fiber orientation and appropriate layer configurations significantly enhance mechanical performance, with notable improvements in maximum stress capacity and strain energy absorption. The findings validate the potential of smart composite systems in advanced precision engineering applications and provide critical insights for optimizing their structural performance through parametric design adjustments.

This study also offers a comparative analysis with Classical Laminate Theory to identify deviations resulting from shear deformation and coupling effects. These results hold promise for applications in aerospace, robotics, and energy systems, where adaptability and structural resilience are essential.

Keywords: Composite beams, Piezoelectric actuators, Finite element analysis, Abaqus, Fiber orientation, Layer configuration

1 Introduction

The integration of smart materials into structural systems marks a transformative advancement in modern engineering, bridging the gap between passive load-bearing designs and adaptive, multifunctional systems. Among these smart materials, piezoelectric actuators have emerged as a cornerstone for applications requiring precision, adaptability, and dynamic response.

[*]Corresponding Author, Professor, Department of Mechanical Engineering, University of Tehran, Tehran, Iran, mahdavin@ut.ac.ir
[†]B.Sc. Student, Department of Mechanical Engineering, University of Tehran, Tehran, Iran, taranehsheidaei@gmail.com
[‡]B.Sc. Student, Department of Mechanical Engineering, University of Tehran, Tehran, Iran, arian26150@gmail.com

Received: 2025/01/18, Revised: 2025/07/19, Accepted: 2025/08/04

Piezoelectric materials exhibit the unique ability to convert electrical energy into mechanical strain and vice versa, enabling simultaneous sensing and actuation functionalities. This dual capability has catalyzed their widespread adoption in aerospace, robotics, automotive engineering, and biomedical devices [1]–[3].

Composite materials are widely recognized for their high strength-to-weight ratio, customizable stiffness, and the ability to tailor mechanical properties to specific design requirements. When integrated with piezoelectric actuators, these smart composites enable multifunctional capabilities such as structural control, vibration mitigation, and energy harvesting. Such composite systems are particularly attractive in aerospace, robotics, and precision engineering, where lightweight adaptability is critical [4], [5]. Among them, piezoelectric laminated beams have garnered significant attention for their ability to translate mechanical deformation into electrical signals and vice versa, thereby enabling both sensing and actuation functionalities.

In aerospace applications, Macro-Fiber Composite (MFC) actuators bonded to helicopter rotor blades have demonstrated vibration amplitude reductions of up to 80% at primary harmonic frequencies (50 Hz), leading to improved ride comfort and extended structural fatigue life [6], [7]. In structural health monitoring (SHM), sensor–actuator networks based on piezoelectric laminates embedded in rotorcraft flex beams have achieved over 95% detection accuracy for delaminations and microcracks, primarily by analyzing dynamic transfer function responses in the 100–500 Hz range [8]. These materials are also advancing energy harvesting systems; bend–twist carbon Fiber laminates integrated with piezo layers have exhibited open-circuit voltages approaching 8 V and energy densities near 0.5 mW/cm³ under low-frequency excitations (30 Hz) [9], [10]. Furthermore, smart panels utilizing piezoelectric actuation have shown 20–25 dB improvements in transmission loss around resonance frequencies, making them viable for active noise and acoustic control [11].

These diverse applications underscore the adaptability of piezoelectric composite beams, where microscale electromechanical effects can be precisely tuned to enable macroscale performance in control, sensing, and energy conversion. However, much of the existing literature is limited to idealized configurations—such as fixed geometries, symmetric stacking sequences, on-axis fiber orientations, or thin-laminate assumptions—and relies heavily on Classical Laminate Theory (CLT). While CLT provides analytical efficiency, it fails to account for critical physical phenomena including transverse shear deformation, bending–twisting coupling, and shifts in the neutral axis. These effects become especially prominent in off-axis plies or multilayer configurations [12]. Moreover, only a limited number of studies benchmarks CLT predictions against high-fidelity finite element models across a wide design parameter space, leaving gaps in our understanding of when classical theory fails [13], [14].

To address these limitations, the present study systematically investigates how two fundamental design parameters—fiber orientation angle and the number of laminate layers—affect the static electromechanical response of piezoelectric composite beams. Unlike prior works, this study utilizes both analytical modeling and detailed finite element simulations in ANSYS to analyze cantilevered graphite/epoxy beams under tip loads and voltage excitation. This combined approach not only validates the general trends predicted by CLT but also reveals the boundaries of its applicability in configurations exhibiting strong coupling effects and geometric asymmetry [15].

Our results demonstrate that aligning fiber orientation with the principal loading axis substantially enhances actuation-induced deflection, which is in agreement with recent investigations on piezoelectric composite optimization [16]. Additionally, while increasing the number of layers generally improves stiffness and electromechanical response, the benefits plateau beyond a certain threshold, highlighting a design trade-off between structural complexity and functional efficiency [17]. These findings offer valuable insights into the design of adaptive structures, where performance, weight, and responsiveness must be finely balanced.

In sum, this study contributes to the broader body of knowledge on smart materials by

quantifying the limitations of classical analytical models and offering validated design guidelines for optimizing piezoelectric composite actuators. The results have direct implications for next-generation systems in aerospace, energy harvesting, and health monitoring, where structural intelligence and adaptability are essential.

2 Theoretical framework

This section presents the theoretical foundations for analyzing composite beams with piezoelectric actuators. The formulations and material properties used herein are primarily based on the classical lamination theory framework presented in Kaw [1]. Specifically, the stiffness matrices, transformed reduced stiffness tensors, and the ABD matrix formulation follow the methodology described in Mechanics of Composite Materials [1].
The composite material employed in this study is graphite/epoxy, well-known for its high strength-to-weight ratio and excellent stiffness. The properties of the composite material, such as Young's modulus (E), shear modulus (G), and Poisson's ratio (ν), are provided in Table (1). These properties are essential inputs for evaluating stiffness matrices and stress-strain relationships.
thus enabling:

$$Q_{11} = \frac{E_1}{1 + \nu_{21}\nu_{12}} \quad (1)$$

$$Q_{12} = \frac{\nu_{12}E_2}{1 + \nu_{21}\nu_{12}} \quad (2)$$

$$Q_{22} = \frac{E_2}{1 + \nu_{21}\nu_{12}} \quad (3)$$

$$Q_{66} = \frac{G_{12}}{1 + \nu_{21}\nu_{12}} \quad (4)$$

$$\Rightarrow Q = 10^9 * \begin{bmatrix} 181.8 & 2.91 & 0 \\ 2.91 & 10.4 & 0 \\ 0 & 0 & 7.2 \end{bmatrix}$$

The transformation matrix, denoted as [T] is essential for converting stresses and strains between global and local coordinate systems. Here, θ represents the fiber orientation angle.

$$T = \begin{bmatrix} cos^2\theta & sin^2\theta & 2sin\theta cos\theta \\ sin^2\theta & cos^2\theta & -2sin\theta cos\theta \\ -sin\theta cos\theta & sin\theta cos\theta & cos^2\theta - sin^2\theta \end{bmatrix} \quad (5)$$

$$\overset{\theta=15^\circ}{\Longrightarrow} T = \begin{bmatrix} 0.933 & 0.067 & 0.500 \\ 0.067 & 0.933 & -0.500 \\ -0.250 & 0.250 & 0.866 \end{bmatrix}$$

$$\overset{\theta=30^\circ}{\Longrightarrow} T = \begin{bmatrix} 0.750 & 0.250 & 0.866 \\ 0.250 & 0.750 & -0.866 \\ -0.433 & 0.433 & 0.500 \end{bmatrix}$$

Using the ABD method (Lamination theory), the force and moment resultants across the laminate are obtained. [A], [B], and [D] are the extensional, coupling, and bending stiffness matrices, respectively.

Table 1 Elastic properties of composite for theory

E_1	E_2	ν_{12}	G_{12}
181 GPa	10.3 GPa	0.28	7.17 GPa

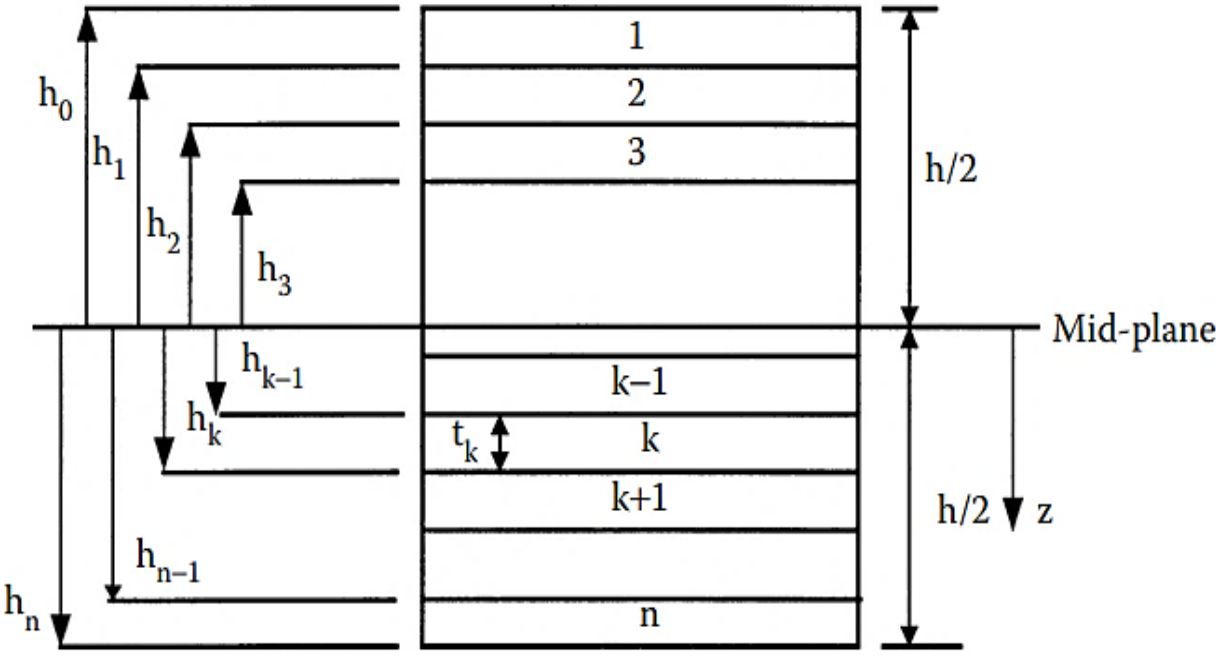

Figure 1 ABD method

$$A_{ij} = \sum_{k=1}^{n} \left[\left(\bar{Q}_{ij}\right)\right]_k (h_k - h_{k-1}), \qquad i = 1,2,3;\ \ j = 1,2,6; \tag{6}$$

$$B_{ij} = \frac{1}{2}\sum_{k=1}^{n} \left[\left(\bar{Q}_{ij}\right)\right]_k (h_k^2 - h_{k-1}^2), \qquad i = 1,2,3;\ \ j = 1,2,6; \tag{7}$$

$$D_{ij} = \frac{1}{3}\sum_{k=1}^{n} \left[\left(\bar{Q}_{ij}\right)\right]_k (h_k^3 - h_{k-1}^3), \qquad i = 1,2,3;\ \ j = 1,2,6; \tag{8}$$

$$\begin{bmatrix} M_x \\ M_y \\ M_{xy} \end{bmatrix} = \begin{bmatrix} B_{11} & B_{12} & B_{16} \\ B_{12} & B_{22} & B_{26} \\ B_{16} & B_{26} & B_{16} \end{bmatrix} \begin{bmatrix} \varepsilon_x^0 \\ \varepsilon_y^0 \\ \gamma_{xy}^0 \end{bmatrix} + \begin{bmatrix} D_{11} & D_{12} & D_{16} \\ D_{12} & D_{22} & D_{26} \\ D_{16} & D_{26} & D_{16} \end{bmatrix} \begin{bmatrix} \kappa_x \\ \kappa_y \\ \kappa_{xy} \end{bmatrix} \tag{9}$$

$$\begin{bmatrix} \varepsilon_x \\ \varepsilon_y \\ \gamma_{xy} \end{bmatrix} = \begin{bmatrix} \varepsilon_x^0 \\ \varepsilon_y^0 \\ \gamma_{xy}^0 \end{bmatrix} + z \begin{bmatrix} \kappa_x \\ \kappa_y \\ \kappa_{xy} \end{bmatrix} \tag{10}$$

ermshe tTε_x^0 and κ_x represent mid-plane strains and curvatures respectivly. Stresses within each layer are computed by substituting these results into the constitutive equations.

$$\begin{bmatrix} \sigma_x \\ \sigma_y \\ \tau_{xy} \end{bmatrix} = \begin{bmatrix} \bar{Q}_{11} & \bar{Q}_{12} & \bar{Q}_{16} \\ \bar{Q}_{12} & \bar{Q}_{22} & \bar{Q}_{26} \\ \bar{Q}_{16} & \bar{Q}_{26} & \bar{Q}_{16} \end{bmatrix} \begin{bmatrix} \varepsilon_x \\ \varepsilon_y \\ \gamma_{xy} \end{bmatrix} \tag{11}$$

3 Numerical simulation and analysis

The objective of this study was to investigate the mechanical behavior of composite beams with integrated piezoelectric actuators, focusing on the effects of fiber orientation and layer configuration on their performance. Finite Element Analysis (FEA) was employed using Abaqus software to simulate and analyze the composite beams under varying conditions.
Initially, composite beams were modeled as three-dimensional deformable structures. The geometry of the beam was standardized with the length, width, and the thickness of 100 mm, 10mm, and 0.5mm for each layer being respectively.
The piezoelectric material used was PZT-5H, a widely recognized piezoelectric ceramic with high electromechanical coupling properties. The composite material was graphite-epoxy, selected for its excellent strength-to-weight ratio and high stiffness. The elastic and piezoelectric properties of these materials were derived from experimental data and existing literature to ensure realistic simulation results.
To ensure the accuracy of the finite element simulations, a refined mesh was generated. A mesh convergence study was conducted using a representative case involving a two-layer laminate with a 0° fiber orientation. As illustrated in Figure 2, both internal work and strain energy were monitored across a range of mesh sizes. The results demonstrated convergence, with both metrics stabilizing as the element size decreased. Based on this analysis, a global element size of 0.0008 mm was selected as an optimal compromise between numerical accuracy and computational cost. This mesh density resulted in stable outputs while maintaining reasonable simulation runtimes. Each model comprised approximately 9,750 three-dimensional continuum elements. To accurately capture the electromechanical behavior, the piezoelectric actuator and composite layers were modeled using appropriate coupled-field solid elements.

Table 2 Elastic properties of composite samples in Abaqus

E1 (GPa)	E2 (GPa)	E3 (GPa)	Nu12	Nu13	Nu23	G12 (GPa)	G13 (GPa)	G23 (GPa)
200	10	10	0	0.25	0	6	5	6

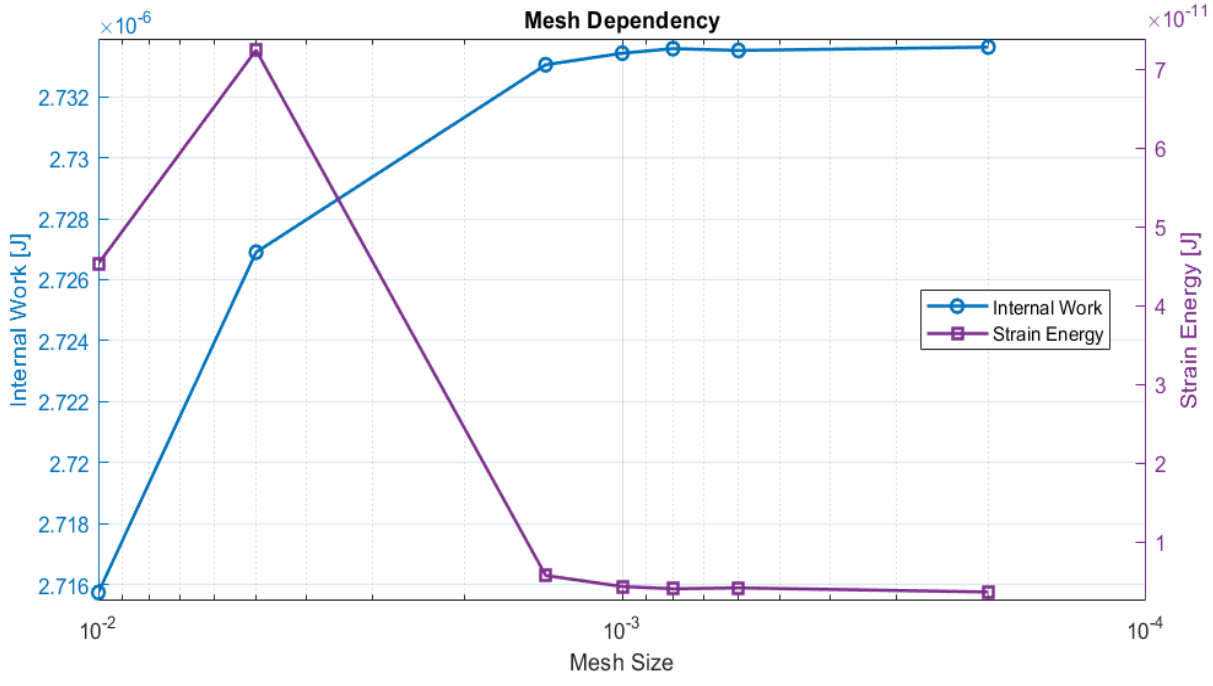

Figure 2 Mesh convergence for a two-layer laminate (0° fiber). Internal work and strain energy stabilize below 0.001 mm, validating the selected mesh size of 0.0008 mm.

The composite beam was modeled with clamped–clamped boundary conditions, where all translational and rotational degrees of freedom were constrained at both ends. For electrical loading, a voltage of 10 V was applied across the thickness of the piezoelectric patch: the bottom electrode (bonded surface) was grounded (0 V), and the top electrode was set to +10 V. This configuration induced a uniform electric field through the thickness, producing in-plane strain via the inverse piezoelectric effect. The patch was assumed to be perfectly bonded to the host laminate, and lateral fringing fields were neglected.

The resulting deformation and stress distribution were recorded under static loading conditions. For the mechanical analysis, a Static General solver was used, with a total simulation time of 1 second. Automatic stabilization was employed with a dissipated energy fraction of 0.0002 to ensure numerical stability during the simulations.

Two parametric studies were conducted to evaluate the effects of design variables on the performance of the composite beams:

A) Variation in Fiber Orientation

The fiber orientation angles were varied from 0° to 90° in increments of 15°, keeping the number of layers constant at 2. This study aimed to evaluate the impact of fiber alignment on the stress-strain behavior, bending resistance, and maximum strength of the beams.

B) Variation in Number of Layers

The number of composite layers was increased from 2 to 6, while keeping the fiber orientation fixed at 0°. This analysis investigated how increasing the structural thickness influenced the beam's mechanical properties, including stiffness, ultimate strength, and strain energy absorption.

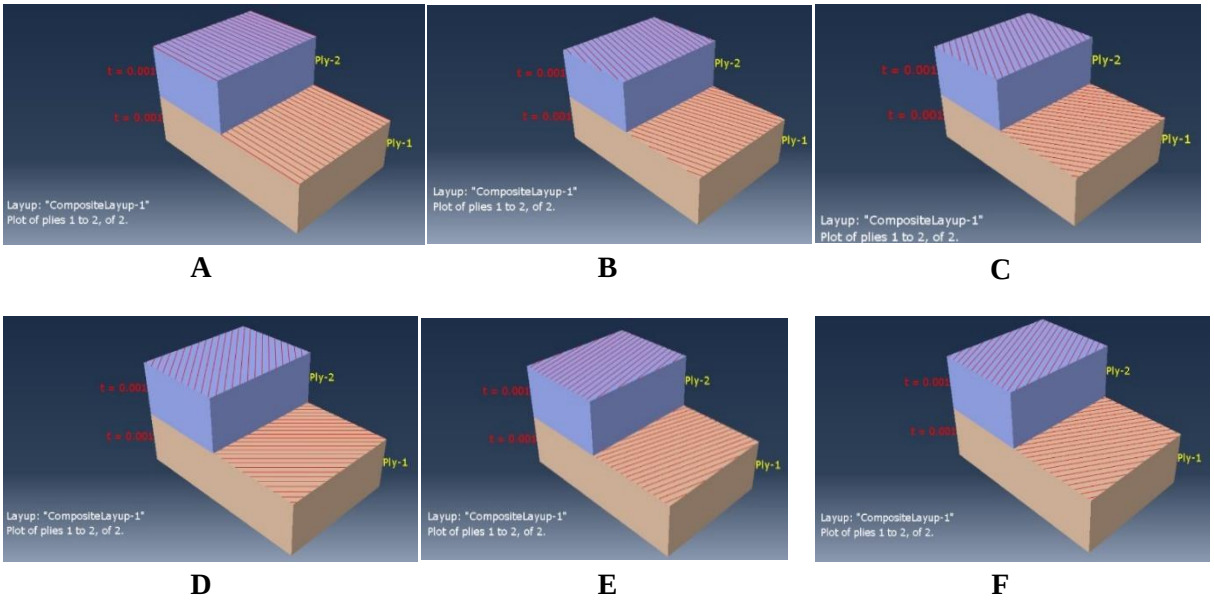

Figure 3 Variation in Fiber Angle: **A**) 0/0, **B**) 15/-15, **C**) 30/-30, **D**) 45/-45, **E**) 60/-60, **F**) 75/-75, **G**) 90/-90

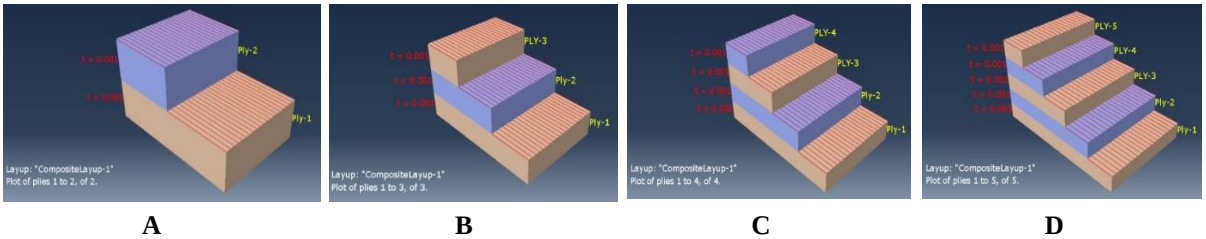

Figure 4 Variation in number of layers; **A**)2, **B**)3, **C**)4, **D**)

The simulations were conducted on an 8-core Intel Core i5 processor, with an average runtime of 9 minutes and 24 seconds per configuration. The computational setup was optimized to balance accuracy and efficiency, ensuring reliable results within a reasonable timeframe.
The simulation outputs included force-displacement data, stress-strain plots, and detailed stress distributions for each configuration. Using these outputs, some analyses were performed. Conversion to Stress and Strain was one of these tasks. Force data was converted to stress values using experimental equation derived for this configuration, while displacement data was converted to strain using geometric relations.

$$\sigma_{B_{exp}} = \frac{3.F.l}{2.b.h^2}$$

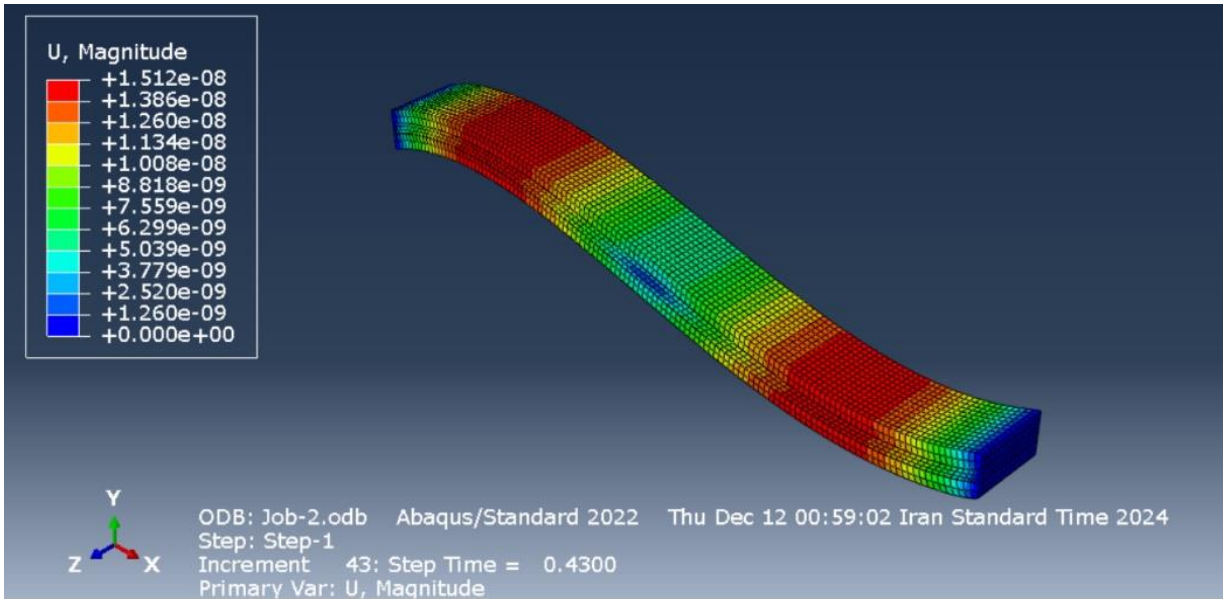

Figure 5 Deformed composite beam

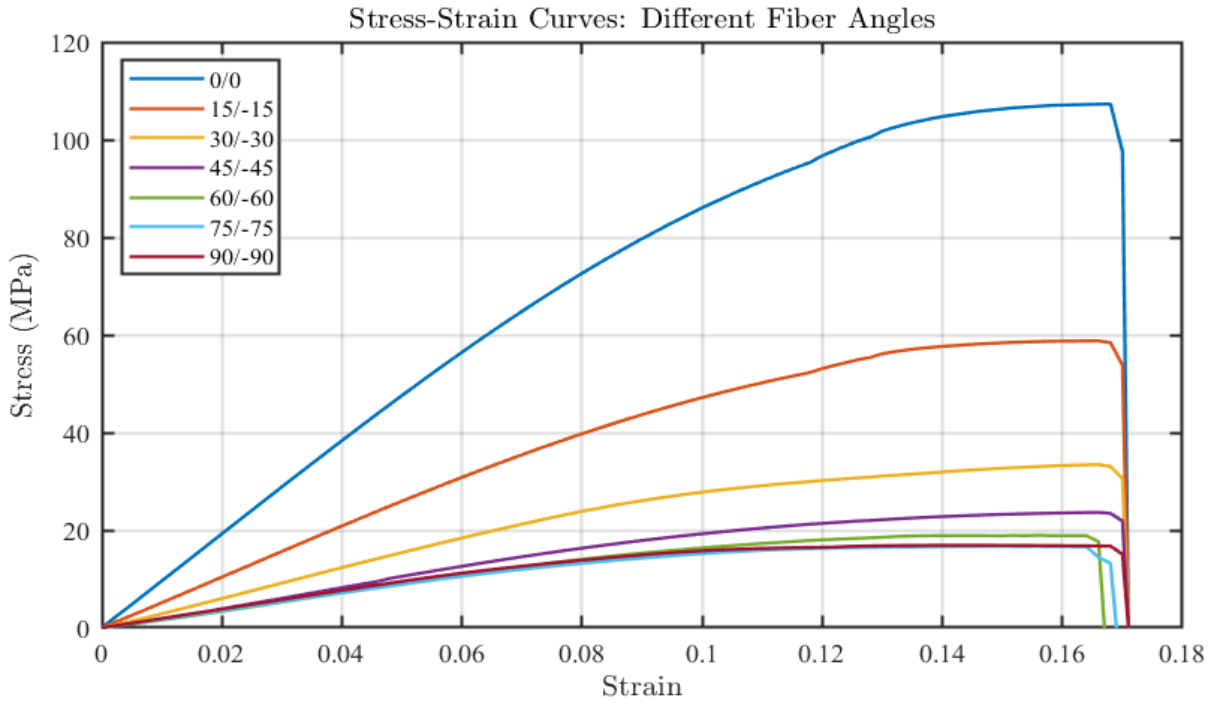

Figure 6 Stress-strain diagram drawn for variation in fiber orientation

Table 3 Final strain and stress values for various fiber orientations

Angle (deg)	Final strain	Final stress (MPa)
0	0.168	107.3055
15	0.166	58.7895
30	0.166	33.4314
45	0.166	23.6430
60	0.162	18.9630
75	0.164	16.6962
90	0.168	16.8912

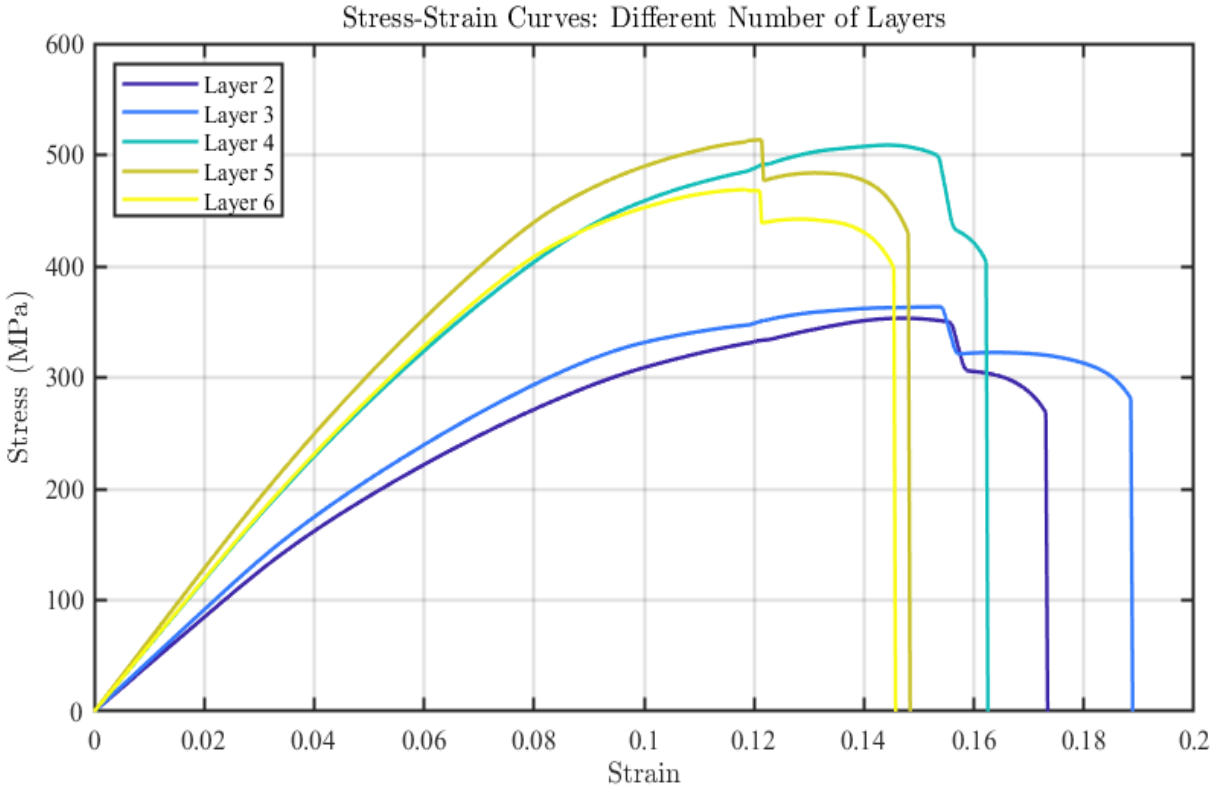

Figure 7 Stress-strain diagram drawn for Variation in number of layers

Table 4 Numerical data of Figure (7)

Number of layers	First fracture strain	First fracture stress (MPa)	Final fracture strain	Final fracture stress (MPa)
2	0.1561	353.244	0.1736	268.548
3	0.1540	363.432	0.1885	280.993
4	0.1449	508.732	0.1627	403.766
5	0.1210	513.488	0.1476	429.503
6	0.1177	469.148	0.1445	398.404

Furthermore, the simulation results were validated against theoretical stress–strain predictions derived from composite beam theory, ensuring consistency and accuracy. And effects of fiber orientation and layer configuration on maximum stress, strain, and bending resistance were analyzed. Nonlinear trends observed in the data were interpreted based on composite mechanics and piezoelectric theory.

4 Results and discussion

4.1 Physical interpretation of parameter effects

Before presenting the numerical results, it is useful to consider how the number of laminate layers and fiber orientation are expected to influence the piezoelectric beam's mechanical response. An increase in the number of layers leads to higher bending stiffness due to the greater second moment of area. According to beam theory, this reduces deflection under the same piezoelectric actuation. However, added layers also increase mass and interlaminar damping, slightly shifting resonance frequencies and improving vibration suppression in dynamic cases.
Fiber orientation affects the stiffness anisotropy of the laminate. When fibers are aligned with the beam axis ($\theta = 0°$), axial stiffness is maximized, minimizing deflection. As the angle increases toward 45°, the effective stiffness decreases, leading to larger bending deformation but also increased coupling effects, such as bending–twisting interaction and shear deformation. These effects are not captured by classical analytical models but are resolved in FEM simulations. Together, these parameters govern how efficiently the piezoelectric patch can induce bending. Understanding their physical influence helps explain the trends seen in the following simulation results and provides a basis for design optimization.

4.2 Effect of fiber orientation on beam performance

The fiber orientation angles were varied incrementally from 0° to 90°, while a constant layer count of two was maintained. The stress–strain plots generated for each angle (Figure 6) revealed significant differences in performance.
At 0°, the beams achieved the highest ultimate stress of 107.31 MPa, indicating optimal load transfer along the fiber axis. As the orientation increased, the ultimate stress exhibited a nonlinear decrease, reaching its minimum value of 16.7 MPa at 75°. However, a slight increase in stress was observed at 90°, likely due to stress redistribution under orthogonal loading conditions.
The strain at failure remained relatively consistent across orientations, suggesting that fiber angle primarily influences stress capacity rather than deformation behavior. The observed nonlinear trend highlights the anisotropic nature of composite materials.

4.3 Comparison of simulation results with theory for fiber orientation

The simulation results were cross-verified with experimental data and theoretical predictions to ensure robustness. Where discrepancies were present, they were analyzed and attributed to material property assumptions or numerical approximations inherent in the finite element model. Discrepancies, where present, were analyzed and attributed to material property assumptions or numerical approximations inherent in the finite element model.
It is observed that maximum performance is at 0° Orientation in which fibers are aligned with the loading direction maximizing stiffness and load-carrying capacity due to efficient stress transfer along the fiber axis. As fiber orientation diverges from the load direction, shear deformation becomes dominant, reducing stress capacity. The observed nonlinear reduction in stress capacity aligns with classical lamination theory, which predicts a rapid decline in stiffness and strength as the angle increases. Also, the trend obeys the initial decrease in stress up to 75° and a slight increase after that.

Table 5 Comparison of simulation results with theory for fiber orientations

Angle	Simulation stress (MPa)	Theoretical stress (MPa)	Error (%)
0/0	107.3	107.3	0.0
15/-15	58.8	63.4	7.9
30/-30	33.4	49.3	47.6
45/-45	23.6	30.7	30.0
60/-60	19.0	27.6	45.7
75/-75	16.7	15.9	-4.6
90/-90	16.9	17.0	2.4

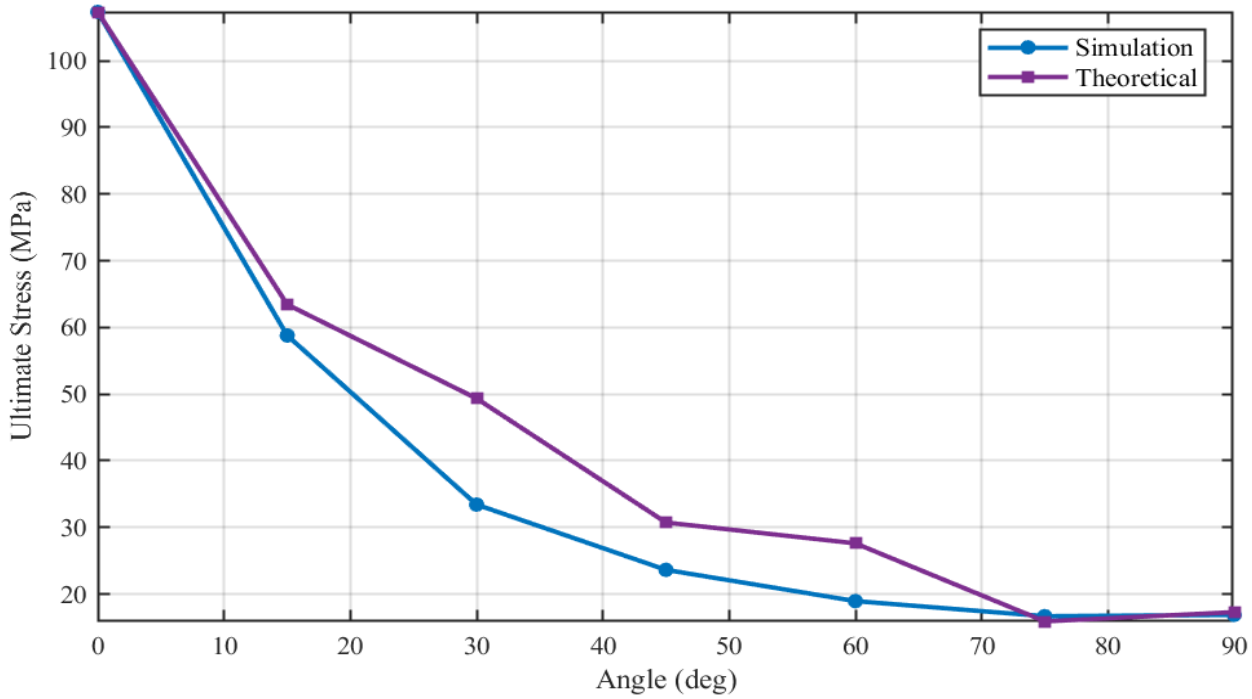

Figure 8 Ultimate stress for different orientations in simulation and theory

While the overall trend between simulation and theoretical stress aligns with expectations, a noticeable deviation appears at mid-range fiber orientations (30°–60°), where the analytical predictions overestimate the stress response by up to 47%. This error can be attributed to the limitations of Classical Laminate Theory (CLT), which neglects bending–twisting coupling and transverse shear deformation. At these off-axis angles, the laminate experiences significant shear compliance and coupled deformation effects, which are naturally captured in the FEM simulation but not in the analytical model. Additionally, minor discrepancies may arise from mesh discretization, localized stress concentrations, and the idealized material property assumptions used in the theoretical formulation. The sudden improvement in agreement at 75° and 90° is consistent with the reduction in coupling effects as fibers re-align closer to the transverse axis, where the structure behaves more like a quasi-isotropic plate in tension. These deviations do not undermine the validity of the model but rather highlight the importance of using FEM in configurations where classical theory assumptions begin to break down. Indeed, for materials at the nanoscale, such as nanocomposites, classical theories may be inadequate, and generalized continuum mechanics approaches are often necessary [18].

4.4 Effect of number of layers on beam performance

The number of layers was varied from 2 to 6, with a fixed fiber orientation of 0°. Results showed a consistent increase in ultimate stress with additional layers, up to five layers, after which the trend plateaued. The strain at failure exhibited an inverse relationship, decreasing as the number of layers increased.
Maximum ultimate stress (429.50 MPa) was achieved with 5 layers, beyond which the stress began to stabilize. Strain at the first fracture decreased from 0.156% for 2 layers to 0.118% for 6 layers, reflecting a reduction in ductility with increased thickness.

4.5 Comparison of simulation results with theory for number of layers

Using the same approach, theoretical values were calculated and compared with the results obtained from the simulations.

Table 6 Comparison of simulation results with theory for several layers

Number of layers	Simulation stress (MPa)	Theoretical stress (MPa)	error (%)
2	268.6	207.3	-22.8
3	281.0	250.4	-10.9
4	403.8	389.3	-3.6
5	429.5	419.4	-2.4
6	398.4	400.5	0.5

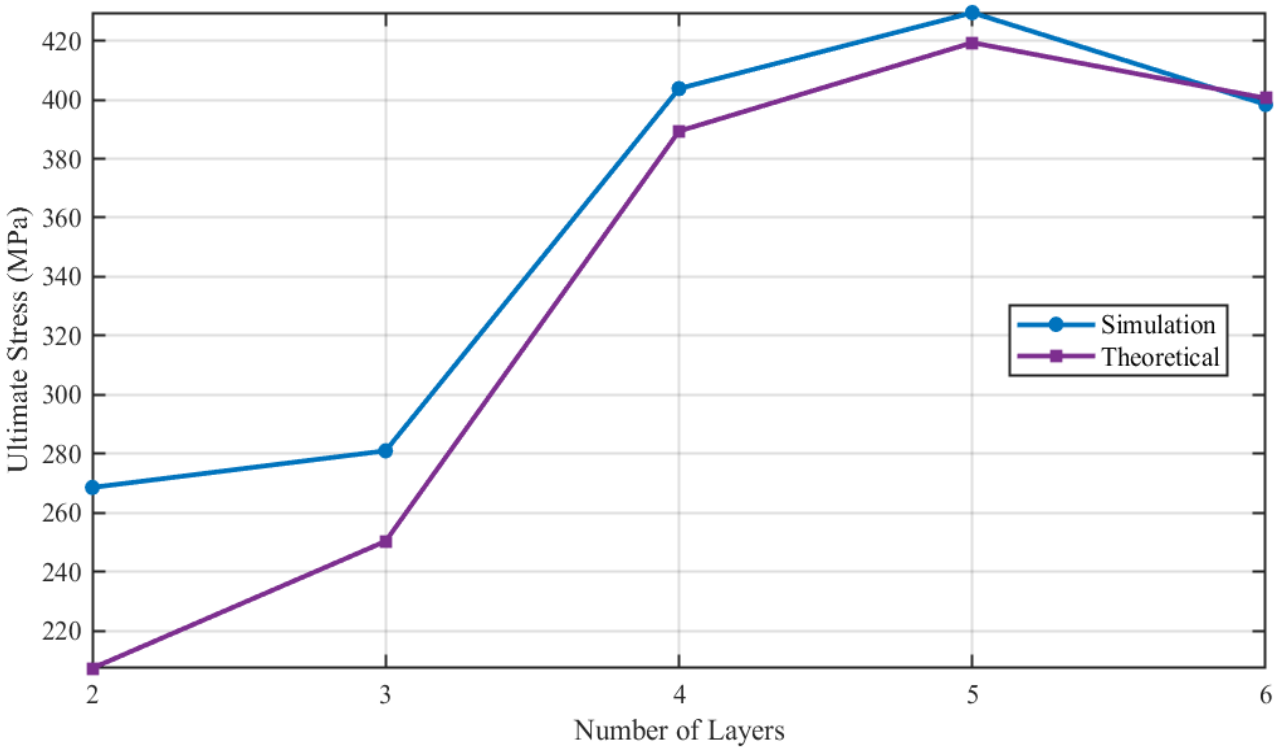

Figure 9 Ultimate stress for various number of layers in simulation and theory

Figure (9) clearly shows that an increase in the number of layers results in enhanced bending stiffness and stress-carrying capacity, as more material contributes to load resistance. But there is a trade-off in ductility. While strength improves with additional layers, the reduction in strain at failure indicates decreased flexibility, a common trade-off in multi-layer composites. The plateau in stress improvement suggests that additional layers contribute less to overall performance due to increased interlaminar shear stresses.
Across all configurations, the simulated stresses closely matched theoretical values. This validation confirms the robustness of the finite element model and its accuracy in capturing the complex interplay of fiber orientation and layer configuration.
There are some potential causes for minor discrepancies. The simplifications in material property inputs may have contributed to minor variations. Also, mesh density and stabilization parameters could have influenced localized stress predictions.
For applications requiring maximum strength, 0° fiber orientation and a 5-layer configuration are recommended. In scenarios prioritizing flexibility, fewer layers may be preferred despite reduced ultimate stress. These findings may guide the design of adaptive composite systems in fields such as aerospace, robotics, and precision engineering.

5 Conclusion

This study investigated the mechanical performance of composite beams integrated with piezoelectric actuators, focusing on the effects of fiber orientation and layer configuration. Through detailed Finite Element simulations in Abaqus, key findings were derived that highlight the interplay between fiber orientation, layer configuration, and structural performance. Composite beams demonstrated optimal mechanical performance when fibers were aligned at 0°, achieving maximum stress capacity and efficient load transfer. A nonlinear reduction in ultimate stress was observed as the fiber orientation angle increased, consistent with the anisotropic behavior of composites.
Increasing the number of layers generally enhanced the ultimate stress capacity and bending resistance, with a notable plateau effect beyond five layers. However, the strain at failure decreased with additional layers, indicating a trade-off between strength and ductility. These findings emphasize the importance of parameter optimization in the design of smart composite systems and align well with classical lamination theory.
The insights gained from this study offer practical guidance for designing adaptive systems in aerospace, robotics, and precision engineering applications, where structural adaptability and performance are critical. Future work could extend this research to dynamic loading scenarios, more complex boundary conditions, and advanced material models to capture nonlinearities and failure mechanisms more accurately. This could include exploring micro or nanoscale composite beams where theories incorporating length scale parameters, such as MCST, become crucial for accurate predictions [19].
This research not only validates existing theoretical models but also provides a foundation for further advancements in the design and application of smart composite systems equipped with piezoelectric actuators.

References

[1] A. K. Kaw, "*Mechanics of Composite Materials*," 2nd Edition, CRC Press, Boca Raton, 2006, https://doi.org/10.1201/9781420058291.

[2] E. F. Crawley, and J. de Luis, "Use of Piezoelectric Actuators as Elements of Intelligent Structures", *AIAA Journal*, Vol. 25, No. 10, pp. 1373–1385, 1987,

https://doi.org/10.2514/3.9792.

[3] C. T. Sun, and X. D. Zhang, "Use of Thickness-shear Mode in Adaptive Sandwich Structures", *Smart Materials and Structures*, OP Publishing Ltd, Vol. 4, No. 3, pp. 202–206, 1995, DOI 10.1088/0964-1726/4/3/007.

[4] A. Erturk, and D. J. Inman, "*Piezoelectric Energy Harvesting*", First Edition, John Wiley and Sons Ltd., Publication, 2011, ISBN: 978-0-4703.

[5] M. Janocha, Ed., "*Adaptronics and Smart Structures: Basics, Materials, Design, and Applications*", Springer, 2007.

[6] J. Sirohi, and I. Chopra, "Fundamental Understanding of Piezoelectric Strain Sensors," *Journal of Intelligent Material Systems Structur*e, Vol. 11, No. 4, pp. 246–257, 2000, doi: 10.1106/44GX-J54A-WMKR-TR4D.

[7] B. K. Stanford, "Aeroelastic Tailoring of Rotor Blades using Distributed Piezoelectric Actuation," *Journal Aircraft*, Vol. 57, No. 4, pp. 629–641, 2020, doi: 10.2514/1.C035571.

[8] Y. Song, A. Ghoshal, J. Harrison, and M.J. Sundaresan, "Damage Detection in Composite Rotorcraft Flexbeams using Active Piezoelectric Sensor Networks," Smart Materials and Structure, Vol. 31, No. 5, 2022, Article No. 055020, doi: 10.1088/1361-665X/ac56f2.

[9] D. Zhu, M. Worthington, and N. J. Grabham, "Energy Harvesting from Bend–twist Coupling in Composite Beams," *Composite Structures*, Vol. 279, pp. 114755, 2022, doi: 10.1016/j.compstruct.2021.114755.

[10] S. R. Anton, and H. A. Sodano, "A Review of Power Harvesting using Piezoelectric Materials," *Smart Materials and Structures*, Vol. 16, No. 3, pp. R1–R21, 2007, doi: 10.1088/0964-1726/16/3/R01.

[11] H. Zhang, S. Das, and S. Adhikari, "Piezoelectric Shunt Damping and Smart Acoustic Metasurfaces," Journal of Sound and Vibration, Vol. 547, pp. 117464, 2023, doi: 10.1016/j.jsv.2023.117464.

[12] M. C. Ray, and S. K. Batra, "Exact Solutions for Piezoelectric Composite Laminates Subjected to Mechanical and Electric Loading," *Advanced Materials and Structures*, Vol. 14, No. 3, pp. 587–597, 2005.

[13] J. Wang, and Y. Zhang, "Comparative Analysis of Analytical and FEM Models of Smart Laminated Composites," *Acta Mechanica*, Vol. 233, pp. 3425–3442, 2022, doi: 10.1007/s00707-022-03253-9.

[14] A. K. Noor, et al., "Modeling and Simulation of Piezoelectric Smart Composite Structures," *Computer Methods in Applied Mechanics*, Vol. 291, pp. 1–24, 2023.

[15] H. Lee, S. Kim, and J. Park, "Analytical and FEM Validation of Static Response in Piezoelectric Laminated Beams," *Journal of Computational and Applied Mathematics*, Vol. 398, pp. 113640, 2022.

[16] A. Akhlaq, et al., “Effect of Piezoelectric Nonlinearity on Bending Behavior of Smart Beams,” *Materials*, Vol. 16, No. 7, pp. 2839, 2023, doi: 10.3390/ma16072839.

[17] M. Ezzraimi, et al., “Static and Frequency Analysis of Functionally Graded Piezoelectric beams,” *Journal of Engineering and Applied Science*, Vol. 70, pp. 92, 2023, doi: 10.1186/s44147-023-00250-4.

[18] N. M. Do, H. V. Le, and T. T. Nguyen, "Static Behavior of Porous FG Nanoplates Reinforced by Graphene Platelets using Quasi-3D Plate Theory," *Advances in Applied NanoBio-Technologies*, Vol. 3, No. 2, pp. 552–563, 2024, doi: 10.1080/17455030.2024.2396335.

[19] M. Wang, G. Zhao, J. Zhang, and Y. Liu, "The Electro-magneto-elastic Analysis of Functionally Graded Piezoelectric Composite Cylindrical Shells Reinforced with Graphene Platelets," *Mechanics of Advanced Materials and Structures*, pp. 1–20, 2024, doi: 10.1080/15376494.2024.2324353.